Journal of Engineering and Sustainable Development
Vol. 29, No. 06, November 2025
https://jeasd.uomustansiriyah.edu.iq/index.php/jeasd
ISSN 2520-0917
Research Article
https://doi.org/10.31272/jeasd.2865

Adsorption of Lead and Cobalt from Aqueous Solution Using Unmodified Date Palm Seeds: Kinetics and Isotherms

Nadia Matter Almhana[1], Rasha Al-Saedi[1*], Ishraq Khudhair Abaas[1], Israa M. Al-Tameemi[2]

[1]Environmental Engineering Departmen, College of Engineering, Mustansiriyah University, Baghdad, Iraq
[2]School of Civil Engineering, Universiti Sains Malaysia, Penang 14300, Malaysia

*Email: rasha.azeez@uomustansiriyah.edu.iq

Article Info

Received	**20/07/2024**
Revised	**08/09/2025**
Accepted	**15/09/2025**

Abstract

The ongoing pollution of water with heavy metals and the costly treatment methods have raised the need to search for an alternative treatment approach. In this work, a batch adsorption experiment using unmodified date palm seeds (UDPS) was conducted to investigate the effects of contact time, pH, adsorbent dose, and initial concentration on the removal rates of cobalt and lead from aqueous solution. Freundlich and Langmuir isotherms, as well as the kinetics of Pseudo-First- and second-order adsorption models, were also assessed. The results showed that equilibrium was reached at a 90-minute contact time, achieving the highest removal efficiencies of Co^{+2} and Pb^{+2} at pH 6, an adsorbent dose of 0.5 g, and initial Co^{+2} and Pb^{+2} concentrations of 10 mg/L, with maximum uptake potentials of 0.9 and 0.89 mg/g, respectively. Lead adsorption fitted slightly better to the Freundlich isotherm than to the Langmuir isotherm, whereas Co adsorption over the Langmuir isotherm. Regarding the kinetics of adsorption, the Pseudo-second order model better represented Co^{+2} and Pb^{+2} than the Pseudo-first-order model. FTIR results illustrate peaks at 3250 cm^{-1} and 3413 cm^{-1} for Co and Pb, respectively, corresponding to O=H stretching mode on the adsorbent surfaces.

Keywords: Adsorbent dose, Contact time, Freundlich, Initial concentration, Langmuir, Pseudo model

1. Introduction

Various and vast amounts of pollutants (particularly heavy metals) are produced daily from industrial activities [1]. In developing countries, about 90% of industrial wastewater is usually discharged into water systems without proper treatment [2]. The disposal of industrial effluents into these systems poses a high risk to human health, plants, microorganisms, and the entire food chain, as heavy metals dissolve immediately within the matrix and are readily available for uptake by living organisms [3]. Some metals, such as cobalt and lead (with concentrations above the permissible drinking water limit), have cumulative toxic effects on the human body [4]. The main side effects of lead are damage to the liver, kidneys, and reproductive system, as well as brain functions and primary cellular processes [5], while weakening heart muscles, hearing loss, vision loss, and cognitive impairment are the adverse side effects of cobalt [4], [6]. According to Iraqi standards, the maximum allowable concentrations of Pb and Co in rivers are 0.01 and 0.03 mg/L, respectively [7].

To avoid the toxic and carcinogenic effects of these non-degradable pollutants on human bodies, they can be removed through chemical and physical techniques such as catalysis, ion exchange, oxidation-reduction, chemical precipitation, and filtration [1]. However, the application of these methods has some limitations, such as sludge production, membrane fouling, high energy costs, and the formation of oxidation by-products, as well as technical and economic issues [8].

Adsorption has been a successful method for reducing pollutants in wastewater. Still, it depends on the selection of the adsorbent (which must have specific chemical and physical properties, as well as environmental safety) [1]. The process occurs when a liquid solute accumulates on the adsorbent's solid surface, forming a molecular or atomic film of adsorbates [8]. In this approach, the molecules of the adsorbate are bound to solid surfaces via a chemical/physical process alongside the mass transfer process [9].

To reduce the disposal of green waste, which costs money to discard, as well as conserve natural resources for future generations through waste recycling (one of the sustainable development objectives), besides the plentiful of agricultural wastes in the environment, the use of these wastes as adsorbents has been recently encouraged [3]. Green or eco-friendly materials have been proven to be efficient adsorbents because they are low-cost, readily prepared, and environmentally friendly, such as walnut shells, coconut tree sawdust [1], grape seeds, lentils, wheat and rice shells, which have been assessed for metal removal from industrial wastewater [8]. Iraq is one of the most significant date producers in the Middle East, with nearly 21 million date palm trees cultivated, yielding around 400,000 tons/year. Globally, millions of tons/day of date pits are wasted due to high date consumption in different regions, as well as their use in biodiesel production and other environmental practices. Date palm seeds as biosorbents have been successfully examined in removing various contaminants from wastewater (in particular, heavy metals). Furthermore, date seed powder can remove traces of toxic elements [2], [4]. Since large amounts of date palm seeds are discarded, they have environmental and economic potential for wastewater treatment [2], [10].

The date palm seed contains 23% hemicellulose, 15% lignin, 57% cellulose, 10-20% crude fibers, 7-10% oil, 5-7% protein, 5-10% moisture, 1-2% ash, 81-83% carbohydrates, and 41-48% oleic acid. They also include total phenols and flavonoids, which have a chelating function. Hence, their chemical constituents qualify them as efficient absorbents [5], [6]. The application of lignocellulosic wastes as adsorbent materials is achieved through the interaction of the adsorbents with functional groups, which can serve as adsorption sites for heavy metal ions. These functional groups are common to all lignocellulosic materials, but their numbers vary depending on the type of material [2]. Cheap lignocellulosic waste materials have effectively removed pollutants from wastewater due to their high porosity and surface area, as well as their resistance to biological degradation. Lignocellulosic materials include three polymers: cellulose, lignin, and hemicellulose. Lignocellulosic wastes also contain small amounts of water, ash, carbohydrates, and organic/inorganic extracts [2].

However, there is a paucity of information regarding the adsorption of heavy metals onto date seeds. Therefore, this work aims to evaluate the removal of toxic metals (cobalt and lead) from aqueous solution using date seed powder under various experimental conditions of pH, contact time, absorbent dose, and initial Pb and Co concentrations.

2. Materials and Methods

2.1. Preparation of Adsorbent

Seeds of date palm (DPS) were obtained from Iraqi markets, stored for a couple of weeks, and then thoroughly washed with tap and distilled water. Seeds of date palm were dried using an oven at 100 °C for 48 hr. The specimens were then ground and sieved to get particle sizes ranging from 0.3 to 0.5 mm. Afterwards, the powder was dried in an oven at 60°C for six hr., and then preserved in a plastic container until use. Table 1 illustrates the physicochemical properties of date palm seeds.

Table 1. Chemical and physical properties of date palm seeds [11]

Components (%)	**Value**
Moisture content	10
Hemicelluse	16.6
Legnin	25
Cellulose	45.8
Protein	5.6
Ash	1.15
Fat	12.7

2.2. Aqueous Solution Preparation

Co(II) and Pb(II) aqueous solutions were prepared by dissolving 44 mg and 26 mg of $CoCl_2$ and $PbCl_2$, respectively (99% purity), in 1000 mL DI water to obtain an initial concentration of 20 mg/L for each Co and Pb. The stock solutions were then diluted with distilled water to the predetermined concentrations (2, 4, 6, 8, 10, 12, 14, 16, and 18 mg/L) using the general dilution formula ($C_1.V_1 = C_2.V_2$) [12].

2.3. Batch Experiment

The experiment was conducted at 25ºC in 250 mL flasks, with shaking at 180 rpm using a magnetic stirrer, and a constant mass of 0.5 g DPS per 100 mL. To find out the equilibrium time of Co (II) and Pb (II) adsorption onto DPS, the experiment was carried out in a batch mode at time intervals of 10, 20, 30, 40, 50, 60, 70, 80, 90, 100, 110, and 120 min at a pH of 6. The effect of pH on the adsorption of cobalt and lead onto DPS was investigated over a pH range of 1-9. The impact of dosage was assessed over a range of 0.1 to 0.7 g/100 mL, with a fixed increment of 0.1 g. The influence of initial Co and Pb concentrations on adsorption performance was also analyzed over a range of 2-18 mg/L. Table 2 presents the constants and variables for the experiments conducted in this work.

Table 2. Parameters and constants used in the batch experiment

Parameter (units)	Range (increment)	Constants for each batch experiment (units)			
		Equilibrium time (minute)	pH	Adsorbent dose (g)	Initial concentration (mg/L)
Contact time (minutes)	10-120 (10)	-	6	0.5	10
pH	1-9 (1)	90	-	0.5	10
Adsorbent dose (g)	0.1-0.7 (0.1)	90	6	-	10
Initial concentration (mg/L)	2-18 (2)	90	6	0.5	-

Based on the preliminary experiment, adsorption reached equilibrium at 90 min. Other parameters (adsorbent dose, pH, and initial concentration) were selected based on the preliminary experiment. After this step, the suspension was filtered using What-man filter paper No.1 in for the purpose of separating the sorbent particles from solution. A 10 mL portion of the solution obtained was then analyzed to determine Co and Pb concentrations, which were measured following the analytical procedures described by Yan and Indra [13] using an atomic absorption spectrophotometer at 510 nm and 450 nm, respectively.

Kinetics and isotherms of Co and Pb adsorption on DPS were examined based on the adsorbent's optimum capacity. Data were summarized by averaging the replicated results. Under equilibrium conditions, the amount of metal adsorbed qe (mg/g) was computed using equation (1) [14]:

$$q_e = \frac{V.\ (C_{in} - C_e)}{m} \quad (1)$$

Where:

Cin: initial concentration of metal (mg/L), Ce: concentrations of metal at an equilibrium state (mg/L), V: volume of aqueous solution (L), W: adsorbent weight (g).

2.4. FTIR Analysis

In this experiment, the spectra of the adsorbent biomass without metals (before adsorption) and with loads of Co (II) and Pb (II) ions (after adsorption) were reported within the range of 400-3400 cm^{-1}, using a Shimadzu spectrometer (FTIR-8400) in the laboratory of Chemistry/ Mustansiriyah University.

2.5. Equilibrium Isotherms and Kinetics

The results of this experiment were also analyzed using the Langmuir and the Freundlich isotherms to describe solute adsorption [14]. An isotherm generally explains the correlation between the adsorbate amount and the equilibrium concentration at a constant temperature [3]. Langmuir isotherm in equation (2) presumes mono-layer coverage, whereas the Freundlich isotherm in equation (3) supposes multi-layer adsorption [15].

$$\frac{c_e}{q_e} = \frac{1}{KL.q_{max}} + \frac{c_e}{q_{max}} \quad (2)$$

$$\ln qe = \ln k_f + \frac{1}{n} \ln Ce \quad (3)$$

Where:

qe: amount of metal ions absorbed at an equilibrium state, (mg/g), Ce: metal ions concentration in the aqueous solution, (mg/L), qm: maximum concentration of metal ions in mono-layer coverage, (mg/g), KL: Langmuir constant, L/mg), and Kf and 1/n: relative adsorption capacity and heterogeneity factor (adsorption intensity) respectively.

In the Langmuir isotherm, qm with KL can be computed from the slope and intercept in Figure 1/qe and 1/Ce. Kf and 1/n in the Freundlich isotherm can be estimated from the same variables in the log qe vs. log Ce graph (Table 3).

The rate of adsorbate uptake onto the adsorbent during the equilibrium time can be described by adsorption kinetics. Kinetics of Pseudo-first and pseudo-second order were employed in this work to assess the adsorption rate constant. The linearity of the plots, as indicated by the correlation coefficient (R2) values (extremely close to unity), confirms that the adsorption process follows one of these kinetic models.

Table 3. Langmuir and the Freundlich isotherm constants for both Co and Pb

Metals	Isotherm constants	Langmuir	Freundlich
Pb	R^2	0.899	0.931
	q_m (mg/g)	0.403	-
	K_L (L/mg)	1.067	-
	K_F	-	1.024
	1/n	-	0.355
Co	R^2	0.962	0.887
	qm(mg/g)	0.384	-
	K_L(L/mg)	1.138	-
	K_F	-	1.013
	1/n	-	0.409

Kinetics of adsorption is often used to interpret adsorption behavior, while the actual mechanism of pollutant transfer is omitted. The linear forms of pseudo-first- and pseudo-second-order kinetics can be illustrated using equations (4) and (5, respectively [8]. For the pseudo-second-order model, the linearized form is based on solid-phase sorption and constants (q_e and K_2), which were computed from the slope and intercept of the graph t/qt vs. t.

$$\frac{dq}{dt} = K1\ (qe - qt) \quad (4)$$

$$\frac{dq}{dt} = K2\ (qe - qt\ )^2 \quad (5)$$

Where:

qe: mass of the adsorbed metal ions at an equilibrium state/ unit weight of adsorbent (mg/g), qt: weight of the adsorbed metal ions at time t (mg/g), and K1 and K2: constants of adsorption ratio for pseudo-first and pseudo-second order models, independently (1/min).

3. Results and Discussion

3.1. Effect of Physicochemical Parameters

In adsorption, the rate of reaction and time to reach an equilibrium status can be elucidated by representing contact time with the percent removal of metal [3], as shown in Fig. 1. The effect of contact time on Co (II) and Pb (II) adsorption was studied at a time range of 10-120 min under experimental conditions of initial Co and Pb concentration 10 mg/L, pH 6, and adsorbent dose 0.5 g/ 100mL. Overall, the percentage removal of Co was quite similar to that of Pb over the whole experimental period. The faster removal efficiency was observed during the first 60 min of the experiment, then slowed between 60 and 90 min, reaching equilibrium at 90 min, with maximum removal efficiencies of 89% and 88% for Co and Pb ions, respectively. Robati et al. [16] investigated the removal of Pb(II) ions from aqueous solutions using carbon nanotubes as adsorbents with an initial concentration of 10 mg/L and an adsorbent dose of 0.05 g. They observed that the lead ion uptake rate declined after 35 min of contact time, due to a decrease in the number of available adsorption sites.

The mechanism can be clarified as follows: the adsorption sites were initially vacant, which encouraged Co and Pb to interact readily with them. Thus, the concentration difference between the solid-liquid interface and the bulk solution was high at the beginning, resulting in higher adsorption during the first 60 min of the experiment. Afterwards, Co and Pb accumulated in the large pores of the adsorbent surfaces, occupying most of the surface binding sites and thereby slowing adsorption [16].

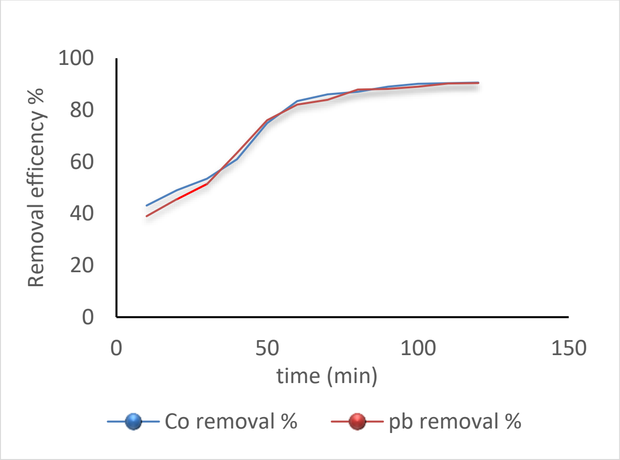

Figure 1. Impact of time on Co^{+2} and Pb^{+2} removal performance using UDPS

sd = 25.97 and 26.28 for Co and pb respectively.

Fig. 2 shows the impact of pH on the removal of Pb^{+2} and Co^{+2} ions in a batch adsorption experiment. The metals removal rate enhanced with the rise in the pH level from 1 to 6, achieving the highest removal rates of 86% and 90% for Co and Pb, respectively at a pH of 6. pH has a considerable impact on the uptake of metal ions since it determines: chemistry of the absorbance surface charge, degree of ionization, and speciation of adsorbate molecules [3]. Increased removal rate at acid conditions, indicating the strong interactions of electrostatic repulsive forces and interference of H^+ ions [8]. However, the removal rates of Co and Pb dropped to 71% and 78%, respectively, when pH increased from 6 to 9. Alkali et al [3] stated that at low pH levels, the number of H_3O ions surpassed that of metal ions, and the adsorbent surfaces were reasonably coated with H_3O^+ ions, which are responsible for the low adsorption. As pH increased up to 6, more H_3O ions migrated to adsorbent surfaces, providing availability of sites to the metal ions, which steadily overlaid onto absorbent surfaces by electrostatic attraction [3]. At pH values > 7.0, adsorption will be limited due to the precipitation of insoluble Co $(OH)_2$ and Pb $(OH)_2$ [8]. This was in agreement with the literature reported by Kowanga et al. [17], who used Moringa oleifera seed powder as an alternative adsorbent for the removal of Pb(II) ions from aqueous solutions. They observed that Pb removal increased sharply from pH 2.0 to 5.5. Therefore, a pH of 5.5 was optimal for high Pb(II) removal under their experimental conditions.

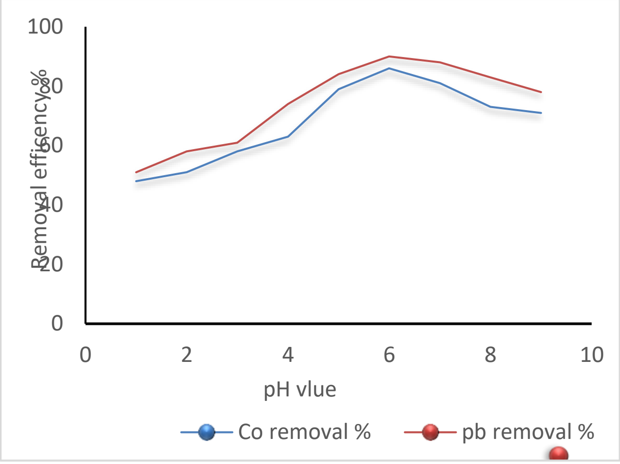

Figure 2. Impact of pH on Co^{+2} and Pb^{+2} removal performance using UDPS

sd = 23.66 and 25.59 for Co and pb respectively.

Adsorbent dosage determines the amount of adsorbent required to remove heavy metals from aqueous solutions [3]. This was achieved in this experiment by varying the amount of adsorbent from 0.1 to 0.7 g/100 mL for both ions under experimental conditions of initial Co and Pb concentrations of 10 mg/L, pH 6, and a reaction time of 90 min. Fig. 3 shows the increase in % removal of Co and Pb with increasing adsorbent dose, approaching 90% and 89%, respectively. Similarly, data were obtained from the literature cited by Almhana et al. [18], who evaluated the removal of cobalt ions from synthetic wastewater using a powder of broad bean peels, with an adsorbent dose range similar to that used in this work. Their results showed an increase in cobalt removal to 98% by increasing the adsorbent amount to 0.5 g/100 mL, after which the adsorption performance approached 98% and then declined, despite raising the dose to 0.7 g/100 mL.

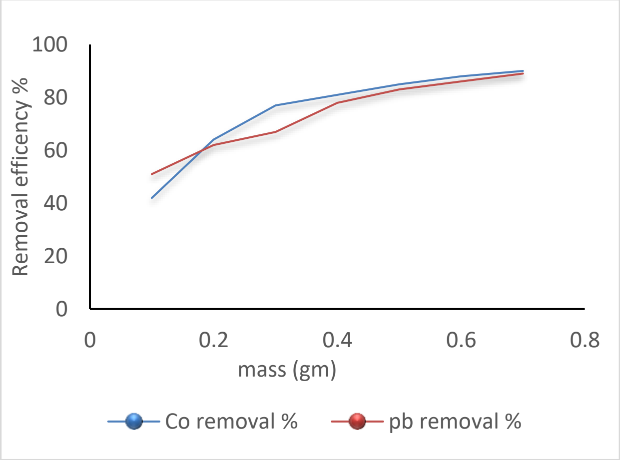

Figure 3. Impact of adsorbent dose on Co^{+2} and Pb^{+2} removal performance using UDPS

sd = 15.78 and 13.02 for Co and pb respectively.

In adsorption processes, the initial concentration is an important parameter, as it provides the driving force to overcome the resistance to mass transfer between the aqueous and solid phases [3]. The batch experiment was carried out at initial Co^{+2} and Pb^{+2} concentrations of 2, 4, 6, 8, 10, 12, 14, 16, and 18 mg/L, a pH of 6, and an absorbent dosage of 0.5 g/100 mL for 90 min. The increased adsorption capacity to about 0.5 mg/g for both Co and Pb ions was recorded with the rise in their initial concentrations from 2 to 18 mg/L (Fig. 4). This could be ascribed to the driving forces of the concentration gradient, which overcame the mass transfer resistance into the adsorbent surfaces [8]. However, Co and Pb removal efficiency decreased from 98% to 81% and 97% to 82% respectively, with the rise in the initial metal concentration from 2 to 14 mg/L Fig. 4, reaching 45% and 44% for Co and Pb respectively at the end of the experiment, owing to the saturation of sorption sites on the adsorbent surfaces [8]. These results were consistent with those of Almhana et al. [18], who investigated cobalt removal from synthetic wastewater using a powder of broad bean peels. Under an initial concentration ranging between 2 and 18 mg/L. When the cobalt concentration ranged from 2 to 12 mg/L, the removal efficiencies ranged from 99% to 91%. Conversely, the removal efficiency declined to 45% once the cobalt concentration was raised to 18 mg/L.

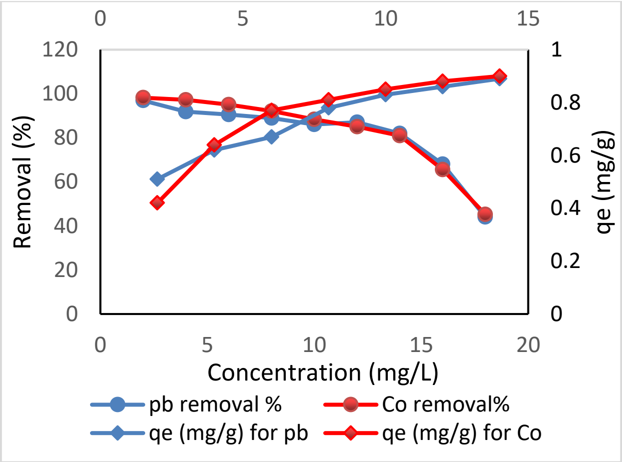

Figure 4. Impact of initial concentration on Co^{+2} and Pb^{+2} removal performance using UDPS.

sd = 0.16 and 0.13 for Co and pb respectively.

In this work, the Freundlich isotherm was slightly preferable to Pb adsorption rather than the Langmuir isotherm, as the determination coefficient (R^2) was marginally higher in the Freundlich isotherm than the Langmuir isotherm Fig. 5, Fig. 6, and Table 3. Additionally, in the Freundlich model, 1/n is less than 1, indicating favorable Pb adsorption on unmodified DPS. However, better Co adsorption was observed from the higher R^2 value of the Langmuir isotherm compared with that of the Freundlich isotherm, indicating chemisorption. This remark was also supported by the closeness of the theoretical values to the experimental data, owing to the homogeneous distribution of active sites on the adsorbent surfaces, indicating a good mono-layer coverage, since the adsorbent that fits the Freundlich model is multi-layer in nature [3].

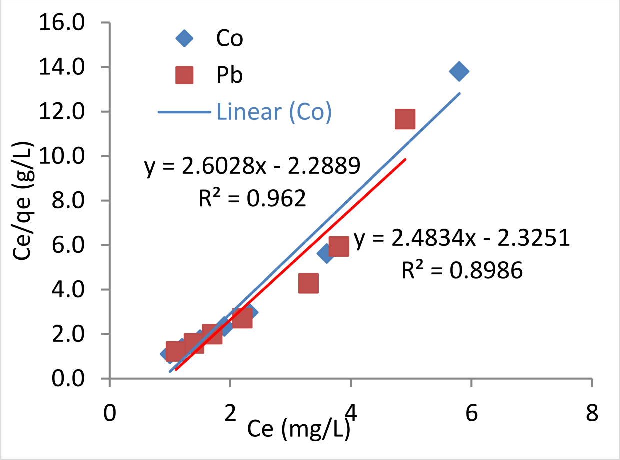

Figure 5. Adsorption of Co^{+2} (blue color) and Pb^{+2} (red color) on UDPS using the Langmuir isotherm

sd = 1.58 and 1.3 for Co and pb respectively.

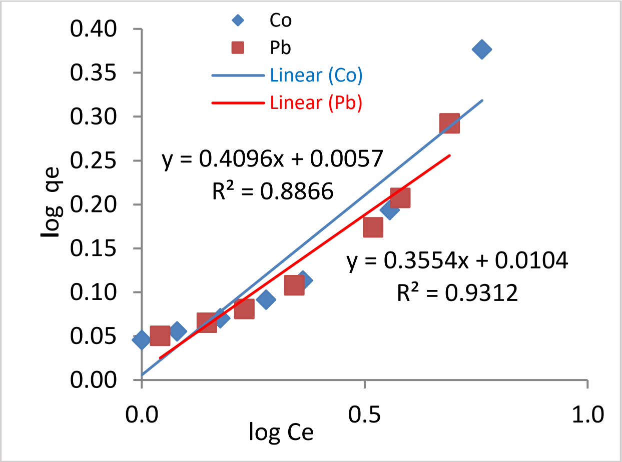

5:

Figure 6. Adsorption of Co^{+2} (blue color) and Pb^{+2} (red color) on UDPS using the Freundlich isotherm
, sd = 0.26 and 0.24 for Co and Pb, respectively

The value of calculated q$_e$ agreed with that of the experimental q$_e$ Table 4, highlighting the fact that this model successfully described the kinetic behavior of Pb adsorption onto unmodified DPS, which was in agreement with Amin et al [8], who used date palm fibers to remove lead from aqueous solution. They concluded that a satisfactory fit of the pseudo-second-order model for Pb and Co adsorption onto the adsorbent supported the presumption that chemisorption is a rate-controlling step that involves the exchange of electrons between the adsorbate and the adsorbent [8].

Table 4, Fig. 7, and Fig.8 show that the correlated R^2 of the pseudo-second-order model is a little greater than that of the pseudo-first-order model, signifying a deep interconnection between the adsorbent and the adsorbate, as both Co and Pb ions are appropriately fitted into the pseudo-second-order kinetic model. Therefore, the pseudo-first-order model is not the best fit for unmodified date palm seeds, as it can only describe adsorption kinetics at the initial stages and cannot fully characterize the adsorption process [3], [19],[20].

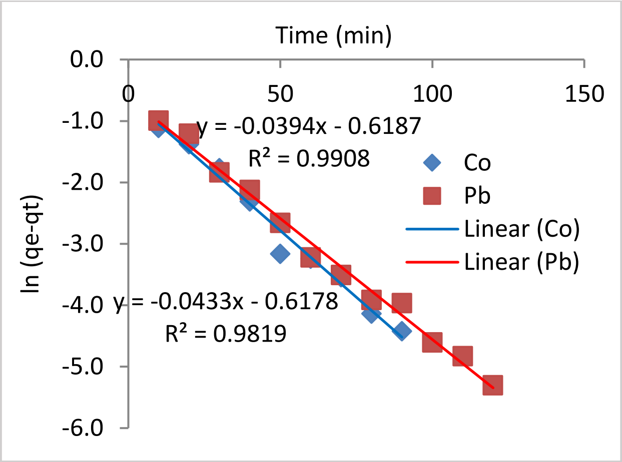

Figure 7. Adsorption of Co^{+2} (blue color) and Pb^{+2} (red color) on UDPS using pseudo-first-order kinetic model sd = 1.11 and 1.37 for Co and pb respectively.

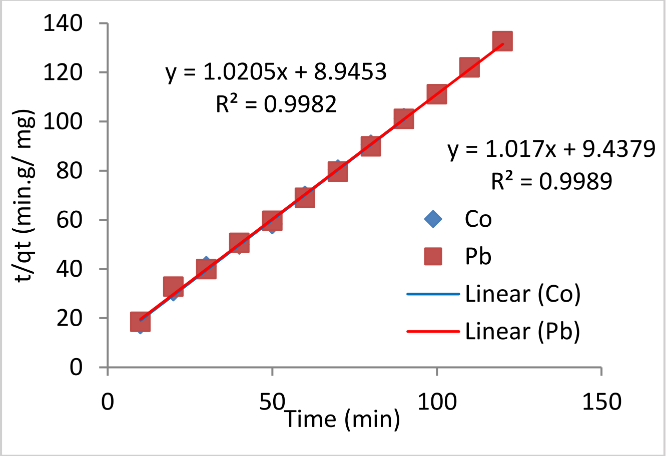

Figure. 8. Adsorption of Co^{+2} (blue color) and Pb^{+2} (red color) on UDPS using the pseudo-second order model

sd = 30.63 and 35.06 for Co and pb respectively.

Table 4. Rates of pseudo-first and second order kinetics for Co and Pb

Metals	Kinetic parameters	Pseudo first order	Pseudo-second order
Pb	q_e (mg/g)	0.240	0.983
	K_1, K_2 (1/min)	0.0394	0.110
	R^2	0.991	0.999
Co	q_e (mg/g)	0.241	0.980
	K_1, K_2 (1/min)	0.0433	0.116
	R^2	0.982	0.998

3.2. Characterizations of Adsorbent Surfaces by FTIR

FTIR spectroscopy is a key tool for identifying various functional groups responsible for adsorption [3], [5]. In this experiment, the spectra of the adsorbent biomass without metals (before adsorption) and with loads of Pb(II) and Co(II) (after adsorption) were reported over the range of 400-3400 cm^{-1}, as shown in Fig. 9 and Fig. 10.

After adsorption, the broad band peaks of UDPS were located at 3250 cm^{-1} and 3413 cm^{-1} for Co and Pb individually, corresponding to the O=H stretching mode of the hydroxyl group. The hydroxyl group is usually found in glucose (an elemental part of the cellulose structure). Similar results were reported by Alkali et al. [3], who used modified and unmodified date peels for the adsorption removal of Pb(II) ions from aqueous solution. They found the broad band peaks (relating to the hydroxyl group), which were close to our results. Peaks were also detected at 2935 cm^{-1} for Co and 2922 cm^{-1}, 2847 cm^{-1} for Pb, characteristic of C=H, ascribed to asymmetric stretching vibration distinctive to aliphatic and aromatic functional groups. The other bands at 1605 cm^{-1} for Co and 1642 cm^{-1} for Pb, likely due to C=O stretching on the adsorbent surfaces. These groups usually form strong surface complexes with metal ions and are part of the cellulose composition [3]. The bands detected at 1451 cm^{-1} for Co and 1521 cm^{-1}, 1429 cm^{-1} for Pb, were ascribed to the presence of alkanes (C=C group), whereas those located at 1249 $cm^{-1}$for Co and 1367 cm^{-1}, 1234 cm^{-1} for Pb, were related to C=N (cyanide group). The broadening and shifting of the bands that appeared at 1053 cm^{-1}, 1022 cm^{-1}, 1083 cm^{-1} for Co and 1086 cm^{-1}, 1055 cm^{-1} for Pb, could be linked to the existence of alcohols, esters, ethers, and carboxylic acids [1]. However, Kowanga et al [17] worked with a powder of Moringa oleifera seeds for the adsorptive removal of Pb ions from an aqueous solution. They detected bands appearing at 1057 cm^{-1} for Pb, which is attributable to the interconnection of Pb ions with the phosphate group.

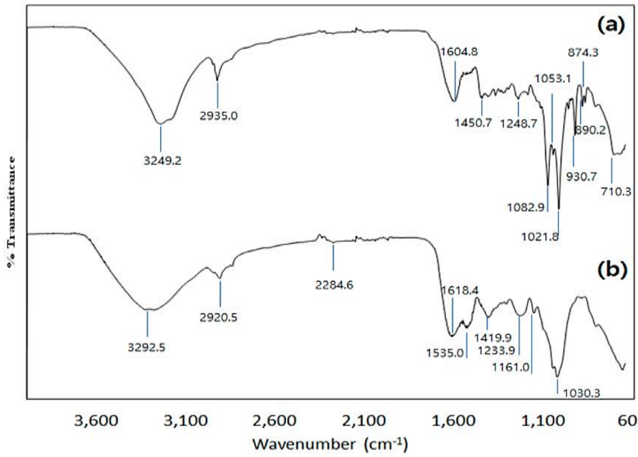

Figure. 9: FTIR of Co, (b) before and (a) after adsorption

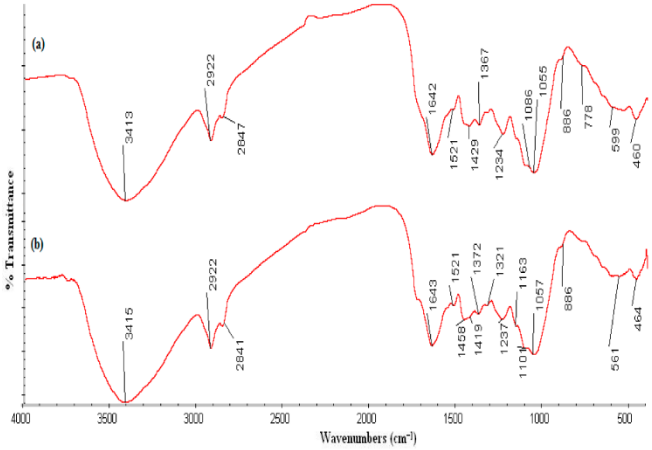

Figure. 10: FTIR of Pb, (b) before and (a) after adsorption

4. Conclusions

This paper demonstrated the application of unmodified date palm seeds as a sustainable adsorbent material to remove Co and Pb from an aqueous solution, using a batch-mode experiment under the following optimum conditions: pH 6, time 90 min, adsorbent dosage 0.5 g, and initial concentration 10 mg/L. The results were also examined using the Freundlich and Langmuir isotherms, and Pseudo-first and second-order kinetics.

No significant changes in Co and Pb removal efficiencies were observed after 90 minutes of the batch experiment, indicating that equilibrium was achieved at 90 minutes of contact time. The greatest Co and Pb removal was observed at pH 6, confirming the interference of H^+ ions. The data on adsorbent dose showed an increase in the Co and Pb removal rates when the dose was raised from 0.1 to 0.5 g. Finally, Co and Pb removal efficiencies dropped by about half when the initial concentrations were increased from 12 to 18 mg/L.

In terms of isotherms, the Freundlich isotherm complied with Pb experimental data (slightly better than Langmuir), whereas Co data better fitted with the Langmuir isotherm. A better fit with Co and Pb data was observed with the pseudo-second-order kinetic model than with the first-order kinetic model.

The infrared spectrum significantly enhanced adsorption efficiency via surface complexation. It also showed a diversity of effective functional groups responsible for lead and cobalt adsorption.

Acknowledgement

The authors would like to express gratitude to Mustansiriyah University (uomustansiriyah.edu.iq), Baghdad, Iraq, for its assistance in this experiment.

Conflict of interest

The authors state that there are no conflicts of interest in the publication of this paper.

Author Contributions Statement

Nadia Matter Almhana proposed the methodology, developed the methodology, analyzed data, and supervised the findings of this work.

Rasha Al-Saedi developed a theory, analyzed data, and found the problem with the statement.

Ishraq Khudhair Abaas arranged and collected the findings of this work.

All authors discussed the results

References

[1]. B. Al-Najar, M. Bououdina, J. J. Vijaya, R. R. Nair, T. Tatarchuk, "Removal of toxins from the environment using date palm seeds," in *Sustainable Agriculture Reviews,* 1st ed., vol. 34, M. Naushad, E. Lichtfouse, Cham, CH: Springer Nature, 2019, pp. 207–245, doi: https://doi.org/10.1007/978-3-030-11345-2_11 .

[2]. M. Nujic, N. Velic, M. Habuda-Stanić, "Application of date-palm fibers for the wastewater treatment," in *Sustainable Agriculture Reviews,* 1st ed., vol. 34, M. Naushad, E. Lichtfouse, Cham, CH: Springer Nature, 2019, pp. 179–191, doi: https://doi.org/10.1007/978-3-030-11345-2_9.

[3]. M. I. Alkali, N. Abdus-Salam, M. R. Abdullahi, E. Ville, M. K. Dikwa, "Adsorption of Cd (II) and Pb (II) ions from aqueous solution using unmodified and modified adsorbents prepared from desert date peels *(Balanites aegyptiaca),"* *J. Sci. Res.*, vol. 2, no. 2, pp. 53–74, Jan. 2023, doi: https://doi.org/10.5281/zenodo.10580462.

[4]. A. A. J. Mohamed, L. A. Vuai, M. Kombo, O. J. Chukwuma," Removal of selected metal ions using powder of seeds of Ajwaa dates from aqueous solution," *J. Anal. Pharm. Res.*, vol. 8, no. 6, pp. 228–232, Dec. 2019, doi: https://doi.org/10.15406/japlr.2019.08.00343.

[5]. A. A. Maki, Z. A. Abdulnabi, B. A. Mahdi, A. M. R. Al-Taee, L. J. M. Al-Anber, "Removal of lead ion from industrial wastewater by using date palm seeds as a low-cost adsorbent," *M. J. M. S.*, vol. 35, no. 2, pp. 51–60, Jul. 2020, doi: https://doi.org/10.58629/mjms.v35i2.21.

[6]. A. N. Ghanim, "Utilization of date pits derived bio-adsorbent for heavy metals in wastewater treatment," *Q. J. E. S.*, vol. 16, no. 1, pp. 58–69, Feb. 2023, doi: https://doi.org/10.30772/qjes.v16i1.910

[7]. B. A. Mahmood, "Environmental properties and analysis of the Euphrates river within Anbar governorate in Iraq: a review," *I. J. D. S.*, vol. 11, no. 2, pp.150–163, Jan. 2021, doi: https://doi.org/10.36531/desert.2022.172742.

[8]. M. T. Amin, A. A. Alazba, M. N. Amin, "Absorption behaviors of copper, lead, and arsenic in aqueous solution using date palm fibers and orange peel: kinetics and thermodynamics," *Pol. J. Environ. Stud.*, vol. 26, no. 2, pp. 543–557, Nov. 2017, doi: https://doi.org/10.15244/pjoes/66963.

[9]. M. A. A. Anuar, M. D. Sharum, N. Sharip, "Removal of copper and cobalt from textile wastewater using date palm as bioadsorbance and implication to pH," *M. A. R. I.*, vol. 4, no. 2, pp. 201–206, Jan. 2023, doi: https://doi.org/10.30880/mari.2023.04.02.027.

[10]. T. Ahmad, M. Danish, M. Rafatullah, A. Ghazali, O. Sulaiman, R. Hashim, M. N. Ibrahim, "The use of date palm as a potential adsorbent for wastewater treatment: a review," *Environ. Sci. Pollut. Res.*, vol. 19, no. 5, pp. 1464–1484, Dec. 2011, doi: https://doi.org/10.1007/s11356-011-0709-8.

[11]. M. Jonoobi, M. Shafie, Y. Shirmohammadli, A. Ashori, H. Z. Hossein abadi, T. J. Mekonnen, "A review on date palm tree: Properties, characterization and its potential applications," *J Renew. Mater.*, vol. 7,

no. 11, pp. 1055‑1075, Nov. 2019, doi: https://doi.org/10.32604/jrm.2019.08188.

[12]. N. Sivarajasekar, J. Prakashmaran, M. Naushad, B. Z. A. Farhan, S. Poornima, S. Sivapriya, V. Gayathri, T. Pradeepika, V. Raghu, S. Sivamani, S. Dharaskar, N. Dhakal, “Recent updates on heavy metal remediation using date stones (*Phoenix dactylifera L.*)-date fruit processing industry waste,” in *Sustainable Agriculture Reviews,* 1st ed., vol. 34, M. Naushad, E. Lichtfouse, Cham, CH: Springer Nature, 2019, pp. 193‑206, doi: https://doi.org/10.1007/978-3-030-11345-2_10.

[13]. J. Yan, E. M. Indra, “Colorimetric method for determining Pb^{2+} ions in water enhanced with non-precious-metal nanoparticles,” *Anal. Chem.*, vol. 84, no. 14, pp. 6122‑6127, Jun. 2012, doi: https://doi.org/10.1021/ac301018y.

[14]. Z. A. Hammood, T. F. Chyad, R. Al-Saedi, “Adsorption performance of dyes over zeolite for textile wastewater treatment,” *Ecol. Chem. Eng. S*, vol. 28, no. 3, pp. 329‑337, Dec. 2021, doi: https://doi.org/10.2478/eces-2021-0022.

[15]. V. H. Hoang et al., “Recycling paper sludge into hydrochar and ZnO nanocomposite for enhanced ammonium adsorption in aqueous solutions,” *RSC Advances*, vol. 15, no. 9, pp. 6634–6651, 2025, doi: https://doi.org/10.1039/d5ra00493d

[16]. D. Robati, “Pseudo-second-order kinetic equations for modeling adsorption systems for removal of lead ions using multi-walled carbon nanotube,” *J Nanostructure Chem.*, vol. 3, no. 1, pp. 1‑6, Jan. 2013, doi: https://doi.org/10.1186/2193-8865-3-55.

[17]. K. D. Kowanga, E. Gatebe, G. O. Mauti, E. M. Mauti, “Kinetic, sorption isotherms, pseudo-first-order model and pseudo-second-order model studies of Cu (II) and Pb (II) using defatted moringa oleifera seed powder,” *J Phytopharm.*, vol. 5, no. 2, pp. 71‑78, Mar. 2016, doi: https://doi.org/10.31254/phyto.2016.5206.

[18]. N. M. Almhana, S. A. K. Ali, S. Z. Al-Najjar, Z. T. Al-Sharify, “Assessment of cobalt ions removal in synthetic wastewater using broad bean peels,” *J Green Eng.*, vol. 10, no. 11, pp. 10157‑10173, Jan. 2020, doi: https://doi.org/10.21608/ejchem.2022.125852.5588.

[19]. R. Sahmarani, S. Net, C. Chbib, M. Baroudi, B. Ouddane, “Elimination of organochlorine pesticides from water by a new activated carbon prepared from Phoenix dactylifera date stones,” *Environ. Sci. Pollut. Res.*, vol. 28, no. 8, pp. 10140‑10154, Oct, 2021, doi: https://doi.org/10.1007/s11356-020-11445-0.

[20]. O. A. Hussain, A. S. Hathout, Y. E. Abdel-Mobdy, M. M. Rashed, E. A. Abdel Rahim, and A. S. M. Fouzy, “Preparation and Characterization of Activated Carbon from Agricultural Wastes and Their Ability to Remove Chlorpyrifos from Water,” *Toxicology Reports*, vol. 10, pp. 146–154, 2023, doi: https://doi.org/10.1016/j.toxrep.2023.01.011